would be random jumping of protons between the two equilibrium sites in the H bonds. A hindered rotation of the H_2SeO_3 and $HSeO_3$ groups (or what amounts to practically the same, a proton interbond motion) could explain the observed second moment data in the paraelectric phase. The relatively large change in the proton second moment on going from the paraelectric phase to ferroelectric phase I indicates a freezing in of both hindered rotation and intrabond proton jumping. The changes in EFG tensors (ψ) at the Na^{23} sites, however, cannot be understood on the basis of proton rearrangements alone. The proton ordering—like the deuteron ordering in D-STSe—is accompanied by a distortion of the Na^+ and SeO_3^- lattice. Unfortunately, there are too many unknown parameters, so that a unique model of ferroelectric phase I cannot be extracted from our data. It should be pointed out, however, that the existence of free O—H groups is excluded on the basis of the infrared spectra. On going from ferroelectric phase I to ferroelectric phase II, the angular dependence of the proton second moments is only slightly changed, but the Na^{23} EFG data indicate a rearrangement of both the hydrogens and the SeO_3^- and Na^+ ions.

Finally, one may add that from the room-temperature EFG tensors at the Na^{23} sites one obtains—using the point-charge model—the following effective charges for the various ions:

$$e_{Na}=e, \quad e_{Se}=1.1e, \quad e_O=-1.0e, \quad \text{and} \quad e_H=0.9e,$$

where e stands for the elementary charge, and an antishielding factor $(1-\gamma_\infty)=6$ was used.

ACKNOWLEDGMENTS

The authors are grateful to Professor J. L. Bjorkstam for several critical discussions. This work was supported in part by the B. Kidrič foundation and by the Federal Council for the Coordination of Research of Yugoslavia.

PHYSICAL REVIEW VOLUME 170, NUMBER 2 10 DECEMBER 1968

High-Temperature Critical Indices for the Classical Anisotropic Heisenberg Model

DAVID JASNOW AND MICHAEL WORTIS*

Department of Physics, University of Illinois, Urbana, Illinois 61801

(Received 15 July 1968)

High-temperature series expansions for the spin-spin correlation function of the classical anisotropic Heinsenberg model are calculated for various lattices and anisotropies through order T^{-8} (close-packed lattices) and T^{-9} (loose-packed lattices). These series are combined and then extrapolated to give the high-temperature critical indices γ (susceptibility), ν (correlation range), and α (specific heat) as functions of anisotropy. Our results are consistent with the hypothesis that the critical indices change only when there is a change in the symmetry of the system, e.g., in interpolating between the Ising and isotropic Heisenberg models, indices remain Ising-like until the system becomes isotropic, at which point they appear to change discontinuously. Previous results for the limiting cases are confirmed and extended.

1. INTRODUCTION

MUCH of the recent study of critical phenomena, both experimental[1] and theoretical,[2] has centered on the determination of and interrelations between the values of the critical indices (exponents), which measure the type and strength of the singular behavior of various physical quantities at the thermodynamic critical point. The most striking fact about the critical indices is their remarkable insensitivity (for fixed dimensionality) to the details of both dynamics and kinematics.[3] It is now appreciated, however, that, within this context of broad similarity, there are small but nonetheless important differences in critical indices between systems with differing dynamics and/or kinematics. Note, as an example, the variation of the high-temperature susceptibility index γ in three dimensions between the spin-$\frac{1}{2}$ Ising model[4,5] ($\gamma\cong1.250$), the

* Alfred P. Sloan Foundation Fellow.

[1] A review of this work, containing extensive references, has recently been given by L. P. Kadanoff, W. Gotze, D. Hamblen, R. Hecht, E. A. Lewis, V. Palciauskas, M. Rayl, J. Swift, D. Aspnes, and J. Kane, Rev. Mod. Phys. **39**, 395 (1967). See also P. Heller, Rept. Progr. Phys. **30**, 731 (1967).

[2] M. E. Fisher, Rept. Progr. Phys. **30**, 615 (1967), which gives extensive references.

[3] More precisely, some of these differences are actually not so small, for example, a change in sign of the interaction (dynamics) of the two-dimensional spin-$\frac{1}{2}$ Ising model on the triangular lattice converts a ferromagnet to a paramagnet having no phase transition [G. Wannier, Phys. Rev. **79**, 357 (1950)]. However, we are emphasizing here the strong parallels between the critical behavior of, for example, the liquid-gas system and the ferromagnet (experimental) or the somewhat weaker similarity (theoretical) of the three-dimensional Ising and Heisenberg models.

[4] C. Domb and M. F. Sykes, Proc. Roy. Soc. (London) **A240**, 214 (1957).

[5] G. A. Baker, Jr., Phys. Rev. **124**, 768 (1961).

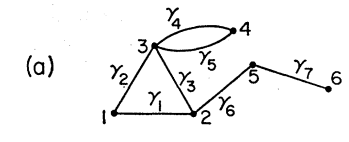

$$\mathfrak{M}_{\alpha\beta}(12) : \frac{1}{2} \sum_{\substack{\gamma_1 \cdots \gamma_7 \\ 3456}} \left(\prod_{i=1}^{7} \eta_{\gamma_i} \right)$$

$$\times V(12)\, V(13)\, V(23)\, V(34)^2\, V(25)\, V(56)$$

$$\times M_3^{\circ}(1;\alpha\gamma_1\gamma_2) M_4^{\circ}(2;\beta\gamma_1\gamma_3\gamma_6) M_4^{\circ}(3;\gamma_2\gamma_3\gamma_4\gamma_5)$$

$$\times M_2^{\circ}(4;\gamma_4\gamma_5) M_2^{\circ}(5;\gamma_6\gamma_7) M_1^{\circ}(6;\gamma_7)$$

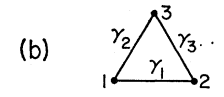

$$\mathfrak{M}_{\alpha\beta}(12) : \sum_{\substack{\gamma_1\gamma_2\gamma_3 \\ 3}} \left(\prod_{i=1}^{3} \eta_{\gamma_i} \right) V(12)\ V(13)\ V\ (23)$$

$$\times M_3(1;\alpha\gamma_1\gamma_2) M_3(2;\beta\gamma_1\gamma_3) M_2(3;\gamma_2\gamma_3)$$

$$G_2(1;\gamma_1\gamma_2) : \frac{1}{2} \sum_{\substack{\gamma_3 \\ 2,3}} \left(\prod_{i=1}^{3} \eta_{\gamma_i} \right) V(12)\ V(13)\ V(23)$$

$$\times M_2(2;\gamma_1\gamma_3)\ M_2(3;\gamma_2\gamma_3)$$

FIG. 1. A reducible graph and its skeleton. (a) A graph and its contribution to $\mathfrak{M}_{\alpha\beta}(12)$ in the unrenormalized theory. (b) The skeleton graph and its contribution to $\mathfrak{M}_{\alpha\beta}(12)$ and $G_2(1;\gamma_1\gamma_2)$ in the renormalized theory.

dynamically different spin-$\frac{1}{2}$ Heisenberg model[6] ($\gamma \cong 1.43$), and in turn, the kinematically different spin-infinity Heisenberg model[7,8] ($\gamma \cong 1.38$). One is led by these observations to the following questions:

(a) How many different types of critical behavior are there, as classified by the critical exponents?

(b) Which features of the dynamics and kinematics of a given system serve to determine its critical exponents and which are irrelevant?

(c) How, physically and mathematically, do the features which *are* relevant exert their influence on the critical indices?

Concerning (c), we have nothing to say other than to point out that the question remains almost entirely open, with the exception of a few exactly soluble models[2] and the crude but appealing "droplet theory."[9] It is the purpose of this paper to explore questions (a) and (b) within the context of the classical (spin-infinity) anisotropic nearest-neighbor Heisenberg model.

The choice of this model is dictated by the following considerations: (i) Variation of the anisotropy parameters allows one to interpolate continuously between a number of dynamically quite different situations. For example,[10] by varying the degree of longitudinal anisotropy, one progresses from the Ising model (longitudinal coupling only) through the isotropic Heisenberg model to the so-called x-y model[11] (totally transverse coupling). In addition, (ii) $S=\infty$ is suggested by convenience. First, as workers on the isotropic Heisenberg model have noted,[8,12,13] the computation of series expansion coefficients becomes simpler in the classical limit, when noncommutation may be neglected.[14] Second, the series once obtained are empirically observed to be smoother (and, thus, more reliably extrapolated) for $S=\infty$ than for finite spin.[15] Finally, (iii) the Ising and Heisenberg limits have been studied previously and constitute a useful check.[16,17]

The anisotropic Heisenberg model has recently been investigated by Dalton and Wood[18] through a correlation function decoupling (random-phase approximation) and via high-temperature series for spin $\frac{1}{2}$ (through order T^{-5}). These authors interpolate with a purely longitudinal anisotropy between the Ising and isotropic Heisenberg limits and conclude that the critical exponents change discontinuously in the isotropic limit—a result previously conjectured by Fisher[19] and which the present work corroborates on the basis of longer and more regular series in the $S=\infty$ case. Obokata, Ono, and Oguchi[20] have independently obtained seven terms in the high-temperature susceptibility series for $S=\frac{1}{2}$ with longitudinal anisotropy only. On the basis of a Padé analysis, they are unable to draw strong conclusions.

---

[6] G. A. Baker, Jr., H. E. Gilbert, J. Eve, and G. S. Rushbrooke, Phys. Rev. **164**, 800 (1967).

[7] G. S. Joyce and R. G. Bowers, Proc. Phys. Soc. (London) **89**, 776 (1966).

[8] H. E. Stanley, Phys. Rev. **158**, 546 (1967); P. J. Wood and G. S. Rushbrooke, Phys. Rev. Letters **17**, 307 (1966).

[9] See Ref. 2, Sec. 9.1. See also M. E. Fisher, Physics **3**, 255 (1967); and F. H. Stillinger, Jr., J. Chem. Phys. **47**, 2513 (1967).

[10] See Sec. 2 for details.

[11] E. Lieb, T. Schultz, and D. Mattis, Ann. Phys. (N.Y.) **16**, 407 (1961).

[12] H. E. Stanley and T. A. Kaplan, Phys. Rev. Letters **16**, 981 (1966).

[13] G. S. Joyce and R. G. Bowers, Proc. Phys. Soc. (London) **88**, 1053 (1966); G. S. Joyce, Phys. Rev. **155**, 478 (1967).

[14] As noted in Ref. 6, there are also simplifications for $S=\frac{1}{2}$. These, however, depend on isotropy in an essential way.

[15] C. Domb and M. F. Sykes, Phys. Rev. **128**, 168 (1962).

[16] Domb and Sykes, Ref. 15, have six terms in the Ising susceptibility series and seven for the specific-heat series for general spin. The best present data for the classical Heisenberg model consists of eight terms (close-packed lattices) or nine terms (loose-packed lattices) for the susceptibility (Joyce and Bowers, Ref. 7, and Stanley, Ref. 8) and specific heat (Joyce and Bowers, Ref. 7). For the spin-S isotropic Heisenberg model, six terms have been derived in the second moment series [M. E. Fisher, in *Critical Phenomena*, edited by M. S. Green and J. V. Sengers (National Bureau of Standards, Washington, D.C., 1966); and R. J. Burford, Ph.D. thesis, University of London, 1966 (unpublished)]. For further references, see Ref. 2 and a comprehensive but older review, C. Domb, Advan. Phys. **9**, 149 (1960).

[17] Second moment series for the $S=\frac{1}{2}$ Ising model have been derived by M. E. Fisher and R. J. Burford, Phys. Rev. **156**, 583 (1967). See, however, Ref. 59.

[18] N. W. Dalton and D. W. Wood, Proc. Phys. Soc. (London) **90**, 459 (1967).

[19] M. F. Fisher, Phys. Rev. Letters **16**, 11 (1966).

[20] T. Obokata, I. Ono, and T. Oguchi, J. Phys. Soc. Japan **23**, 516 (1967).

The present work proceeds according to the following plan: Section 2 discusses the Hamiltonian of the model and outlines the derivation of high-temperature, zero-field series expansions in powers of T^{-1} (inverse temperature) for the susceptibility (χ), the second moment of spatial correlations[17] (μ_2), and T times the zero-field specific heat ($C_{H=M=0}$) to order T^{-8} (close-packed lattices) and T^{-9} (loose-packed lattices). These quantities are expected to have singular behavior as $T\to T_c^+$:

$$\text{(a)}\quad \chi\sim(T-T_c)^{-\gamma},$$
$$\text{(b)}\quad \mu_2\sim(T-T_c)^{-(2\nu_1+\gamma)},$$
$$\text{(c)}\quad C_{H=M=0}\sim(T-T_c)^{-\alpha}. \qquad (1.1)$$

Section 3 describes the methods of extrapolation used to extract the critical indices[21] γ, ν_1, and α from the high-temperature series. In Sec. 4, we present our results for various lattices and anisotropies. In Sec. 5, these results are summarized and briefly discussed.

In view of the considerable number of lattices, anisotropies, and different values of the critical exponents which will be considered, it will perhaps prove useful to summarize here our conclusions as they relate to the questions (a) and (b) posed at the outset. For the classical three-dimensional anisotropic Heisenberg model, we find that our results are consistent with the following hypothesis: *The high-temperature critical indices are correlated in a one-to-one manner with the symmetry group of the order parameter in the ground-state manifold*[22] ($T=0$, zero field). For example, at $T=0$ the magnetization of the *isotropic* Heisenberg ferromagnet is free to point in any direction, while the magnetization of the Ising or x-y models have, respectively, an up-down or planar-rotation degree of freedom only. We therefore expect and, in fact, find different critical indices for these three cases.

No exact results are available for our model concerning the thermodynamic properties of the low-temperature phase; however, it is plausible to assume that the symmetry of the order parameter in the low-temperature phase ($T<T_c$, zero field) is the same as its symmetry at $T=0$. If this is so, then the hypothesis stated above correlates the critical indices with the symmetry of the ordered phase.

2. FINDING THE SERIES COEFFICIENTS

The Hamiltonian of the spin-infinity (classical) anisotropic Heisenberg model is

$$-\beta H=\sum_{1,\alpha} b_\alpha(1)S_\alpha(1)+\tfrac{1}{2}\sum_{1,2,\alpha}\eta_\alpha v(12)S_\alpha(1)S_\alpha(2), \qquad (2.1)$$

where numerical arguments stand for lattice sites and are summed over the entire lattice,[23] while the Greek index α stands for the Cartesian components x, y, z. The classical spin vector $\mathbf{S}(1)=[S_x(1), S_y(1), S_z(1)]$ has unit magnitude. $\mathbf{b}(1)$ is the dimensionless magnetic field at site 1. The dimensionless exchange interaction $v(12)=\beta J(12)$ measures the coupling strength between sites 1 and 2. The pure numbers η_α are anisotropy parameters. In computation we will always specialize to the case of zero field and nearest-neighbor interactions,

$$\begin{aligned} v(12)&=v, && \text{1 and 2 nearest neighbors}\\ &=0, && \text{otherwise},\\ \mathbf{b}(1)&=0, && \text{all sites 1.} \end{aligned} \qquad (2.2)$$

Familiar limiting forms of the Hamiltonian (2.1) are

(a) $\eta_x=\eta_y=\eta_z=1$, classical isotropic Heisenberg model (Refs. 8, 12, 13),

(b) $\eta_x=\eta_y=0$, $\eta_z=1$, spin-infinity Ising model (Ref. 15),

(c) $\eta_x=\eta_y=1$, $\eta_z=0$, classical x-y model.

We will study in detail the interpolating forms

(d) $0\leq\lambda=\eta_x=\eta_y\leq\eta_z=1$, prolate anisotropy, interpolates between (a) and (b);

(e) $1=\eta_x=\eta_y\geq\eta_z=\lambda\geq 0$, oblate anisotropy, interpolates between (a) and (c). (2.3)

The thermodynamic behavior of the system follows from the partition function

$$Z[v,\{b\}]=\mathrm{Tr}e^{-\beta H}=\int\prod_1 d\Omega_1 e^{-\beta H}, \qquad (2.4)$$

where the trace for the classical system reduces to a simple integral over solid angle for each unit spin vector. Thermodynamic averages are calculated as

$$\langle X\rangle\equiv Z^{-1}\,\mathrm{Tr}e^{-\beta H}X. \qquad (2.5)$$

In the absence of interaction,

$$Z[v=0,\{b\}]\equiv Z_0[\{b\}]=\prod_1(4\pi)[\sinh|\mathbf{b}(1)|/|\mathbf{b}(1)|], \qquad (2.6)$$

and all correlation functions involving two or more distinct sites factor.

A particularly important quantity in our formulation is the spin-spin correlation function,

$$\mathfrak{M}_{\alpha\beta}(12)\equiv\langle S_\alpha(1)S_\beta(2)\rangle-\langle S_\alpha(1)\rangle\langle S_\beta(2)\rangle$$
$$=[\delta^2/\delta b_\alpha(1)\delta b_\beta(2)]\ln Z, \qquad (2.7)$$

[21] For a review of the definitions of the critical indices see Refs. 1 and 2. Following Ref. 17, we distinguish between the true and effective correlation ranges, whose divergences as $T\to T_c^+$ are characterized by the critical indices ν and ν_1, respectively. Scaling implies $\nu=\nu_1$, a result which for the $S=\frac{1}{2}$ Ising model is exact in two dimensions and confirmed numerically in three.

[22] Notice that, since our model is classical, elementary arguments suffice to determine its ground state for a variety of anisotropies and lattices. See Sec. 4 and Appendix B.

[23] We take the lattice to be cyclically connected, so there is complete translational invariance.

which becomes diagonal in α and β for $T \geq T_c$ (the critical temperature) and $\mathbf{b}=0$. Under the condition (2.2) we calculate (2.7) as a power series in v, the coefficients of which are, of course, functions of the anisotropy parameters η_α. Once the spin-spin correlation function is known, we can immediately form power series for the physical quantities to be studied[12,24,25]:

$$\chi_\alpha = \sum_2 \mathfrak{M}_{\alpha\alpha}(1, 2) = \chi_\alpha(\eta_x, \eta_y, \eta_z), \tag{2.8a}$$

$$\mu_2{}^\alpha = \sum_2 | r_1 - r_2 |^2 \mathfrak{M}_{\alpha\alpha}(1, 2), \tag{2.8b}$$

$$C_\alpha = \tfrac{1}{2} z v^2 \eta_\alpha (d/dv) \mathfrak{M}_{\alpha\alpha}(1, 1+\delta), \tag{2.8c}$$

where z is the number of nearest neighbors and δ is a nearest-neighbor lattice vector. The zero-field dimensionless susceptibility χ_α measures the linear response of the α component of the magnetization per site to a homogeneous magnetic field in the α direction. $\mu_2{}^\alpha$ is the second moment of $\mathfrak{M}_{\alpha\alpha}(12)$ and is a measure of the range of correlations.[17] C_α is the α contribution to the dimensionless specific heat per site at zero field, $C_{M=H=0} = \sum_\alpha C_\alpha$.

To calculate the spin-spin correlation function $\mathfrak{M}_{\alpha\beta}(12)$, we have used a diagrammatic expansion developed by Englert and others[26] in the context of the Ising model. We present here without proofs an outline of our procedure for computing $\mathfrak{M}_{\alpha\beta}(12)$. The interested reader is referred to the literature for further discussion.[26,27] There are two forms of the expansion, bare and renormalized. We have used the renormalized expansion; however, for pedagogical reasons, we give both here.

Define "bare semi-invariants" by

$$M_l{}^0(1; \alpha_1 \cdots \alpha_l) = [\delta^l / \delta b_{\alpha_1}(1) \cdots \delta b_{\alpha_l}(1)] \ln Z_0[\{b\}]. \tag{2.9}$$

Consider a particular connected graph G of n lines and p vertices. Take two of the vertices to be fixed (external) and label them by the lattice points 1 and 2. Label the remaining p-2 (internal) vertices 3, 4, $\cdots$, p in some arbitrary manner. Label each line in the graph by a Cartesian index γ. Let l_i denote the number of lines terminating in the vertex i. Assign to each such graph a contribution to $\mathfrak{M}_{\alpha\beta}(12)$ according to the following rules.

Rule A

(i) For each line write a factor $\eta_\gamma v(ij)$, where i, j are the end points of the line and γ is its Cartesian label.

(ii) For each *internal* vertex (e.g., 3) assign a factor $M_{l_3}{}^0(3; \gamma_1 \cdots \gamma_{l_3})$, where γ_i, $i=1, \cdots, l_3$, are the Cartesian labels of the lines terminating in 3.

(iii) Assign to the two external vertices factors of $M_{l_1+1}{}^0(1; \alpha\gamma_1 \cdots \gamma_{l_1})$ and $M_{l_2+1}{}^0(2; \beta\gamma_1 \cdots \gamma_{l_2})$.

(iv) Sum freely the Cartesian label of each line over all directions and the lattice label of each internal vertex over all lattice sites.

(v) Divide the result of (iv) by the symmetry factor g of the graph in question. g is the order of the symmetry group of the graph under permutation of lines and internal points.[28]

(vi) To find $\mathfrak{M}_{\alpha\beta}(12)$, sum the contributions according to the above rule of all topologically distinct graphs with the two fixed vertices 1 and 2.[29]

An example of a graph and its associated contribution to $\mathfrak{M}_{\alpha\beta}(12)$ is shown in Fig. 1(a).

In a uniform magnetic field the semi-invariants are independent of lattice site (although, of course, they still depend on the Cartesian indices). Thus, on specializing to the nearest-neighbor, zero-field situation (2.2), each graph G contributes a term of the form

$$(v^n/g) C[1, 2; G] \sum_{\{\gamma\}} \Big(\prod_{\text{vertices}} M^0 \Big) \Big(\prod_{\text{lines}} \eta_\gamma \Big), \tag{2.10}$$

where $C[1, 2; G]$ is the number of nonzero terms in the lattice sum A(iv) for fixed Cartesian labels γ. $C[1, 2; G]$ is just the "embedding constant"[30] of the graph G with fixed points 1 and 2, i.e., the number of ways that the graph G can be embedded in the lattice with its external vertices on fixed sites 1 and 2, all internal vertices on lattice sites, and each line along a nearest-neighbor bond. It is important to note at this point that the lattice sums in Rule A (iv) are free, i.e., two or more vertices may fall on the same lattice site. Thus, our "free" embedding constants are not those of Ref. 30. A method of computing the free embedding constants will be presented elsewhere.[31]

The unrenormalized expansion described above is straightforward, but the number of contributing graphs increases very rapidly in high orders. It is more convenient in practice to perform a selective resummation which eliminates all "reducible graphs."[31] A *reducible graph* in this context is a graph containing one or more parts (not containing either of the fixed points 1 or 2) which can be separated from the rest of the graph by cutting at a single point. Such parts are called *reducible parts*. Where a graph has been simplified by cutting away all its reducible parts, the remainder is called a *skeleton*. Skeletons are by construction *irreducible*. For example, Fig. 1(a) is reducible, having Fig. 1(b) as its irreducible skeleton.

[24] In writing (2.8) we have made use of the simplifications which occur for $T > T_c$ and under conditions (2.2).

[25] H. E. Stanley, Phys. Rev. **158**, 537 (1967).

[26] F. Englert, Phys. Rev. **129**, 567 (1963); C. Bloch and J. S. Langer, J. Math. Phys. **6**, 554 (1965).

[27] D. Jasnow, Ph.D. thesis, University of Illinois, 1968 (unpublished). M. Wortis, D. Jasnow, and M. Moore (to be published).

[28] See F. Englert, Ref. 26, Appendix A.

[29] When the lattice points 1 and 2 are the same, there is an additional contribution $M_2(1; \alpha\beta)$ [see Eq. (2.11) below].

[30] See, for example, the review by Domb, Ref. 16, and M. F. Sykes, J. W. Essam, B. R. Heap, and B. J. Hiley, J. Math. Phys. **7**, 1557 (1966).

[31] D. Jasnow, M. Moore, R. Simpson, and M. Wortis (to be published). Actually only the irreducible graph embedding constants are needed (see below).

By lumping together all graphs belonging to the same skeleton, one arrives at a renormalized prescription[26,27] for calculating $\mathfrak{M}_{\alpha\beta}(12)$.

Rule B

Rule B is the same as Rule A with the following exceptions:

(a) Replace M_l^0's by M_l's (to be defined below) in A(ii) and (iii).

(b) To find $\mathfrak{M}_{\alpha\beta}(12)$, sum over all topologically distinct *irreducible* graphs[32] in A(vi).

An example is provided by Fig. 1(b). The renormalized semi-invariants M_l are obtained in terms of self-energy parts[33] G_n. $G_n(1;\alpha_1\cdots\alpha_n)$ is computed by considering irreducible graphs with one fixed, external vertex (labeled 1), into which come n lines with fixed Cartesian labels $\alpha_1\cdots\alpha_n$. All additional lines and vertices are given dummy labels. Each graph contributes according to Rule C.

Rule C

(i) Same as A(i).

(ii) For each internal vertex (e.g., 3) assign a factor $M_{l_3}(3;\gamma_1\cdots\gamma_{l_3})$.

(iii) To the vertex 1 assign a factor unity.

(iv) Sum freely over all dummy labels.

(v) Divide the result of (iv) by g', the symmetry factor for the graph with *one* fixed point.

(vi) To find $G_n(1;\alpha_1\cdots\alpha_n)$, sum contributions from all topologically distinct irreducible graphs with *one* fixed point 1 into which come n lines labeled $\alpha_1\cdots\alpha_n$.

The relation between M_l and the G_n's is given by

$$M_l(1;\alpha_1\cdots\alpha_l) = \left[\exp\left(\sum_{n=1}^{\infty}\sum_{\gamma_1\cdots\gamma_n} G_n(1;\gamma_1\cdots\gamma_n)\frac{\delta^n}{\delta b_{\gamma_1}(1)\cdots\delta b_{\gamma_n}(1)}\right)\right] \times M_l^0(1;\alpha_1\cdots\alpha_l), \quad (2.11)$$

where the derivatives act only on the M_l^0. Now, the G_n's depend on the interaction $v(ij)$ and the M_n's, so that (2.11) has the form of a nonlinear equation determining the M_l's in terms of the M_n^0's and the interaction. The observation that G_n is at least order v^n allows (2.11) to be solved iteratively in powers of v at high temperatures.

The graphical simplification of Rule B carries with it the necessity of calculating the G_n graphs (Rule C) and unscrambling (2.11). In practice the limiting factor in our calculation was the rapid proliferation of graphs in higher orders.[34] The M_l's were obtained in analytic form to $O(v^7)$ as functions of the parameters η_α. These were fed (along with graphs, symmetry factors, and embedding constants) into a computer program which evaluated M_l's to $O(v^8)$ and carried out the calculation of Rule B and the subsequent summations (2.8). This program ran on an IBM 7094 and took roughly three minutes per set of anisotropy parameters per lattice type. We have obtained series for the triangular lattice, the three cubic lattices, and the spinel. Results for the fcc lattice are presented in detail in Sec. 4; in Appendix A the series for χ and μ_2 are presented for several combinations of the η_α. The series for other lattices are somewhat less regular (particularly the two-dimensional lattices); therefore, it is more difficult to form reliable estimates of critical exponents.

Careless errors tend to creep into this sort of graphical expansion. Our series agree with available series in the Ising[15] and isotropic Heisenberg[7,8] limits. In addition our methods apply with only trivial modifications[35] to the Ising model with arbitrary spin. We have checked with available $S=\frac{1}{2}$ Ising series.[17] These checks are quite comprehensive for the following reasons:

(a) All components of $\mathfrak{M}_{\alpha\beta}(12)$ show up in the susceptibility (2.8a); thus, a check of χ_α checks the complete $\mathfrak{M}_{\alpha\beta}(12)$.

(b) Once a lattice was chosen, the only input variables were the η_α. Hence, a check of the series for one set of anisotropy parameters provides a check on the whole program.

In addition, there are internal checks. A fairly strong check is to calculate $\langle \mathbf{S}(1)^2\rangle \equiv 1$ as a power series in v. Terms of first order and higher must vanish.

3. ANALYSIS OF SERIES

Suppose[36] $F(v)$ is one of the functions to be studied (χ, μ_2, $C_{H=0}$); it is known through a finite number of terms in its expansion,

$$F(v) = \sum_{l=0}^{L} f_l v^l + R(v), \quad (3.1)$$

where

$$R(v) = \sum_{l=L+1}^{\infty} f_l v^l$$

[32] Stanley, Ref. 25, lists necessary graphs for loose-packed lattices to order v^9 and close-packed lattices to order v^8. He calculates correlation functions for the isotropic classical Heisenberg model, but his method does not apply to the anisotropic case.

[33] The G_n's are analogs of the mass operator of many-body theory; M_l^0 and M_l are analogs of bare and renormalized propagators; Eq. (2.11) is an integral form of the Dyson equation, and the whole procedure of going from Rule A to Rule B is simply a progagator renormalization.

[34] Through 8th order on the close-packed lattice one needs 71 graphs for the G_n's and 202 graphs for the spin-spin correlation function.

[35] Appropriate changes in the unrenormalized semi-invariants are all that is required.

[36] The methods of analysis as presented in this section apply to series for the close-packed lattices. The series for the loose-packed lattices require slight modification of the methods presented. The basic principles are the same, however. See, for example, Ref. 4 and Stanley, Ref. 8.

is the unknown remainder. The circle of convergence of the series for $F(v)$ passes through the singularity (or singularities) of the function which lie nearest the origin. In addition, the nearest singularity in the physical region[37] of the v plane will generally be identified with the critical point. In the series analyzed, the known coefficients are all positive, indicating (if the trend continues) that a singularity at $v=v_c$ on the positive real axis is on the circle of convergence.[38] It is assumed[4] that the coefficients f_n have the asymptotic form

$$f_n \sim A(1/v_c)^n n^g, \qquad \text{as } n\to\infty, \tag{3.2}$$

since, by Appell's comparison theorem,[39] (3.2) implies

$$F \sim B/(v_c-v)^{1+g}, \qquad v\to v_c^- \quad \text{(along real axis)}, \tag{3.3}$$

for $g>-1$.[40] All available evidence[1,2] indicates that (3.3) is the form taken by the quantities represented by F.

Analysis of the series essentially reduces to fitting the asymptotic behavior of the coefficients to the form (3.2), which is the starting point of the ratio test analysis.[4] Forming the ratios

$$\rho_n \equiv f_n/f_{n-1}, \tag{3.4}$$

we take Eq. (3.2) literally; this suggests that for large n, the asymptotic behavior of ρ_n is

$$\rho_n \sim (v_c)^{-1}[1+(g/n)+O(1/n^2)], \qquad n\to\infty. \tag{3.5}$$

The leading dependence on $1/n$ yields the familiar result that if one plots the numbers ρ_n versus $1/n$, the limiting straight line through the points intersects the $1/n=0$ axis at the critical point $1/v_c=kT_c/J\equiv t_c$, and the limiting slope is g/v_c. The rapidity with which the ρ_n settle down to linear behavior is indicative of the approach to the asymptotic form (3.3). There are numerous examples of this type of extrapolation in the literature.[2,4]

A. Neville Table

To aid in the extrapolation procedure we form the Neville Table[41] (N.T.). The construction of the table for an arbitrary sequence $\{z_n\}$ is demonstrated. The sequence of linear extrapolants $\{l_n^{(1)}\}$, quadratic extrapolants $\{l_n^{(2)}\}$, etc., are formed by

$$l_n^{(0)} \equiv z_n,$$
$$l_n^{(p)} = p^{-1}[n l_n^{(p-1)} - (n-p) l_{n-1}^{(p-1)}], \qquad p=1, 2, \cdots. \tag{3.6}$$

The number $l_n^{(p)}$ is just the intercept at the $1/n=0$ axis of the curve of pth degree drawn through the $p+1$ successive points z_n, z_{n-1}, $\cdots$, z_{n-p}, with $\{z_n\}$ considered a function of $1/n$. The sequences $\{l_n^{(p)}\}$ are displayed in a tabular form called the Neville Table. The various sequences give estimates for the extrapolation to $1/n=0$ of the sequence $\{z_n\}$ allowing for curvature of successively higher degree. For example, if

$$z_n = z'(1+a/n+b/n^2), \qquad \text{for all } n,$$

the sequences $\{l_n^{(2)}\}$, $\{l_n^{(3)}\}$, $\cdots$ would all be constant and equal to z'. If b were positive, the sequence $\{l_n^{(1)}\}$ would monotonically increase toward the value z'.

B. Finding the Critical Point

There are two basic methods used to extrapolate to the value of $t_c=1/v_c$ for a given series $F(v)$. The first is to form the N.T. for the sequence $\{\rho_n\}$. Then, as described in the example above, each sequence of extrapolants should tend to the value $1/v_c=t_c$, as defined in Eq. (3.5). If higher-order terms in $1/n$ are not important in (3.5), then the early sequences should provide a good estimate of $1/v_c$. An example of this type of N.T. for the series $\chi_z(0, 0, 1)$ is shown in Table I.

If one has an estimate g' for the value g appearing in Eq. (3.2), then one can form the sequence of estimates $\{t_n\}$ for t_c, where

$$t_n = n\rho_n/(n+g'). \tag{3.7}$$

The second method for extrapolating the value $t_c=1/v_c$ is then to form the N.T. for the sequence $\{t_n\}$. The sequence of extrapolants should again approach t_c.

C. Evaluating the Critical Index

Two basic methods are used to determine the critical index g defined in Eq. (3.2). Given an estimate $t_c'=1/v_c'$ to t_c, the sequence of estimates $\{g_n\}$ to g can be formed, where[4,42]

$$g_n = n[(\rho_n/t_c')-1]. \tag{3.8}$$

From Eq. (3.5) $\{g_n\}\to g$ as $1/n$ if the estimate t_c' is good.[43] Then one can form the N.T. for the sequence

TABLE I. Neville Table for $\{\rho_n\}$ from $\chi_z(0, 0, 1)$. Entries are estimates of t_c.

n	ρ_n	$l_n^{(1)}$	$l_n^{(2)}$	$l_n^{(3)}$
2	3.8000			
3	3.7263	3.5789		
4	3.6804	3.5428	3.5066	
5	3.6503	3.5299	3.5105	3.5132
6	3.6292	3.5234	3.5106	3.5106
7	3.6135	3.5194	3.5093	3.5076
8	3.6014	3.5168	3.5091	3.5087

[37] The physical region corresponds to positive temperature. Hence, if the exchange interaction $J>0$, the positive real axis of the v plane is the physical domain.

[38] E. C. Titchmarsh, *The Theory of Functions* (Oxford University Press, London, 1939), Chap. 7.

[39] P. Dienes, *The Taylor Series* (Dover Publications, New York, 1957).

[40] For g a negative integer, F has logarithmic behavior. For $g<-1$ the singular part of F behaves as in (3.3). See Ref. 2.

[41] D. R. Hartree, *Numerical Analysis* (Oxford University Press, London, 1952). See also Ref. 6.

[42] C. Domb and M. F. Sykes, J. Math. Phys. **2**, 63 (1961).

[43] This means that $|t_c-t_c'|/t_c \ll 1/L$, where L is the number of terms available in the series for $F(v)$. This is usually satisfied in practice.

$\{g_n\}$. An example of this type of N.T. is shown in Table II for the same case $\chi_z(0, 0, 1)$.

It is felt that a method for finding g which does not rely on a choice of t_c should be used as a check. The procedure, due to Stanley,[8] is to form the sequence $\{g_n\}$, where

$$g_n = n[(\rho_n/l_n^{(1)}) - 1]. \tag{3.9}$$

The number $l_n^{(1)}$ is given by Eq. (3.6) with $\{\rho_n\}$ in place of the general sequence $\{z_n\}$. Then Eq. (3.5) implies that $\{g_n\} \to g$ as $1/n$. The extrapolation is performed by forming the N.T. for the sequence $\{g_n\}$. The method is good if the early variations in the series are not too large; that is, if $\{l_n^{(1)}\}$ converges smoothly and quickly to t_c. This procedure is not successful, therefore, if $\{\rho_n\}$ shows a high degree of curvature.[44] In general, the method is useful in determining trends in the series.

D. Specific Methods for the Second-Moment Series

Two other techniques were used to reduce the second-moment-series data. Recalling that $\mu_2 \sim (T-T_c)^{-(2\nu_1+\gamma)}$, it is advantageous to form a series involving only ν_1.[17] To do this one need only divide the series, $R(v) = \mu_2(v)/\chi(v)$. Then $R(v)$ has the asymptotic behavior

$$R(v) \sim (v_c - v)^{-2\nu_1}$$

and is studied by the methods described above. Alternatively,[17] one may form the sequence $\{\langle r^2\rangle_n\}$, where

$$\langle r^2\rangle_n \equiv b_n/a_n,$$

with b_n the coefficient of v^n in the second-moment series and a_n the coefficient of v^n in χ. Recalling the asymptotic behavior assumed for the $\{a_n\}$ and $\{b_n\}$, the generating function

$$Q(v) \equiv \sum_n \langle r^2\rangle_n v^n \sim (1-v)^{-(2\nu_1+1)}, \qquad v \to 1^-.$$

The important feature here is that $Q(v)$ has radius of convergence equal to unity. This allows an estimate of $(2\nu_1)$ without knowledge of v_c or γ. The series $Q(v)$ may be studied by the methods described above, as if the critical point were known exactly. As a final consistency check, the series for[45]

$$(d/dv)\ \ln Q(v)$$

has been formed for several cases. Each coefficient is then an estimate of the quantity $2\nu_1+1$.

TABLE II. Neville Table for $\{g_n = (\gamma-1)_n\}$ from $\chi_z(0, 0, 1)$ using Eq. (3.8) with $t_c' = 3.509$.

n	g_n	$l_n^{(1)}$	$l_n^{(2)}$	$l_n^{(3)}$
2				
3	0.1858			
4	0.1954			
5	0.2014	0.2252		
6	0.2055	0.2261	0.2278	
7	0.2085	0.2262	0.2266	0.2250
8	0.2107	0.2263	0.2264	0.2260

[44] That appears to be the case for the second-moment series.
[45] D. S. Gaunt, Proc. Phys. Soc. (London) **92**, 150 (1967).

E. Method of Padé Approximants

The method of Padé Approximants[5,46] has been used to support results from the ratio tests. Best results came from using the value of v_c from the ratio tests as input in the Padé analysis. The Padé results were fairly consistent with results of the other methods.

F. Comments

We have dealt at length with the methods used to extract information from the series. The series analyzed in this paper converge more slowly to their asymptotic behavior than one is used to in Ising-model studies, and the presence of curvature is the norm rather than the exception. The N.T. is a good way to perform the extrapolation[47] under these conditions. Systematizing the extrapolation procedure by means of the N.T. is therefore felt warranted.

The use of N.T.'s is definitely not a cure-all. When series are regular but, for example, the ρ_n sequence is curved (as indicated by linear extrapolants), the N.T. helps one estimate the limit point of the sequence. When there is a change in trend, for example, in the $\{\rho_n\}$ or in one of the sequences derived from it, the N.T. must be used with care in conjunction with the usual $1/n$ plot. Also, the $\{l_n^{(p)}\}$ for the larger values of p are not reliable, as they depend on the early terms in the sequence. The early terms reflect the behavior of the system far from the critical region.

4. RESULTS

This section presents in detail the results of series analysis for the fcc lattice. A careful analysis was also done on the bcc series and gave the same critical indices as the fcc except where specifically mentioned below. The bcc series are somewhat more difficult to extrapolate reliably;[48] consequently, the corresponding confidence limits for bcc results are larger than fcc in a

[46] See for example, G. A. Baker, Jr., in *Advances in Theoretical Physics*, edited by K. A. Brueckner (Academic Press Inc., New York, 1965), Vol. I.
[47] An alternative way to take account of some curvature is the "n-shift method." See, for example, Ref. 2. We have used this method as a cross check. Results are consistent with the ones quoted.
[48] One finds for the bcc series a marked alternating behavior superimposed on what appears to be a smooth trend. See Ref. 36. This is presumably a reflection of the enhancement of antiferromagnetic behavior due to the sublattice structure: For loose-packed lattices under conditions (2.2), the free energy is invariant under the replacement $v \to -v$. Under the same replacement the ferromagnetic physical (staggered) susceptibility goes into the antiferromagnetic staggered (physical) susceptibility. The very plausible additional assumption of a unique critical point leads one to suppose (for example, in the case of the ferromagnetic physical susceptibility) that there is, at $v = -v_c$ on the circle of convergence, a singularity due to the (weak) anomaly in the *antiferromagnetic* physical susceptibility. While this additional singularity is always asymptotically dominated by the stronger singularity at $v = v_c$, it nevertheless slows the approach to the limit.

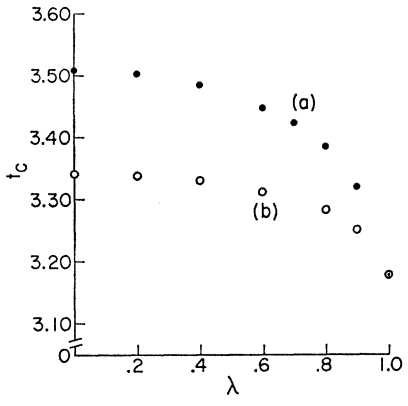

FIG. 2. The critical temperature $t_c = kT_c/J$ versus anisotropy λ for the fcc lattice in the case of (a) prolate anisotropy and (b) oblate anisotropy. See Eqs. (2.3d) and (2.3e).

ratio of roughly 3 to 2. Series for the triangle, simple cubic, and spinel lattices are quite irregular and do not allow precise estimation of critical exponents from the number of terms which we have derived. There is no indication that these lattices would *not* support our general fcc and bcc conclusions, if sufficient terms were available to estimate their asymptotic behavior.

For a given set of anisotropy parameters (η_x, η_y, η_z), there is a choice of which component χ_α, μ_2^α, C_α to study. In practice we will concentrate on the component which yields the most regular and strongly singular series. For example, for $\eta_x=\eta_y=0$, $\eta_z=1$ ($S=\infty$ Ising model), the quantity χ_z is analogous to the usual Ising-model static susceptibility, which for $S=\frac{1}{2}$ in three dimensions behaves as $(T-T_c)^{-5/4}$. On the other hand, $\chi_x=\chi_y$ is similar to the $S=\frac{1}{2}$ Ising-model static perpendicular susceptibility, which is a much more weakly singular quantity, thought to behave like the energy density.[49] "Prolate" and "oblate" anisotropy were defined in (2.3d) and (2.3e). Other cases which do not fall directly into these classes will be defined in terms of the anisotropy parameters (η_x, η_y, η_z).

A. Critical Point

Figure 2 shows a plot of kT_c/J as a function of λ for both prolate and oblate cases, as obtained from susceptibility and second-moment series. The curve for the prolate case is qualitatively similar to the one presented by Dalton and Wood[18] for the $S=\frac{1}{2}$ anisotropic Heisenberg model in the random-phase approximation. For the three limiting cases, λ=0, 1 [see Eq. (2.3d) and (2.3e)], T_c decreases as the symmetry of the Hamiltonian increases from up-down (Ising) through planar rotation (x-y model) to complete rotational invariance (isotropic Heisenberg). For both prolate and oblate cases, as λ increases from zero to one, the increase of the "disordering" component of the Hamiltonian causes T_c to decrease.

[49] M. E. Fisher, J. Math. Phys. **4**, 124 (1963).

For λ in the range $0 \leq \lambda \lesssim 0.6$ and for λ=1, the series are very smooth and kT_c/J is given to within confidence limits[50] of ±(0.10–0.15%). For $0.6 \lesssim \lambda < 1$ the series become more difficult to analyze. The sequences $\{\rho_n\}$ [defined in (3.4)] for the susceptibility series seem to develop a point of inflection, making it very difficult to extrapolate the latest trends. We take this as evidence that in this region the series have not yet fully settled down to their asymptotic behavior. One might say that, as $\lambda \to 1^-$, it takes the system more and more interaction bonds (i.e., more and more powers of λ) to "realize" that it is not isotropic. All things considered, we set confidence limits of ±(0.2–0.3)% for $0.6 \lesssim \lambda < 1$.

B. Indices γ and ν_1

In this section the values of the indices γ and ν_1 are presented as a function of anisotropy. For the cases of prolate and oblate anisotropy γ and $2\nu_1$ are shown for various values of λ in Table III. In the former case the indices refer to χ_z and μ_2^z and in the latter, to χ_x and μ_2^x. The values of the indices for several typical cases in which all three parameters (η_x, η_y, η_z) differ in magnitude and/or sign are shown in Table IV. In each instance the indices apply to χ_α and μ_2^α, where the Cartesian component α is listed. Except in cases explicitly noted to the contrary, the confidence limits are ±1%.[51]

The results in Table III suggest that, as far as the critical indices are concerned, the isotropic Heisenberg limit, λ=1, is singular. For both prolate and oblate anisotropy γ and $2\nu_1$ remain nearly constant for $0 \leq \lambda \lesssim 0.6$, dip slightly in the region $0.6 \lesssim \lambda < 1$, and shoot up to the isotropic Heisenberg value very close to

TABLE III. Indices γ and $2\nu_1$ for prolate and oblate anisotropy.[a]

	Prolate case $\lambda=\eta_x=\eta_y \leq \eta_z=1$		Oblate case $1=\eta_x=\eta_y \geq \eta_z=\lambda$	
λ	γ	$2\nu_1$	γ	$2\nu_1$
0	1.23	1.25	1.32	1.34
0.2	1.23	1.25	1.32	1.34
0.4	1.23	1.25	1.32	1.34
0.6	1.24	1.25	1.32	1.34
0.7[b]	1.21	1.23	1.30	1.32
0.8[b]	1.19	1.20	1.28	1.31
0.9[b]	1.19	1.20	1.28	1.30
1.0	1.38	1.40	1.38	1.40

[a] Unless otherwise noted, confidence limits are ±1%.
[b] No confidence limits given; series not showing asymptotic behavior.

[50] Of course, no statements can be made about the uncertainty in the true T_c or the true critical indices on the basis of series of finite length. The numbers given reflect the *apparent* smoothness of the series and the *apparent* consistency of various different extrapolation procedures, *as based on the number of terms which we have available*. Even where the series are smooth, there is always the hidden hypothesis that the series are long enough for the true asymptotic behavior to have set in. We refer to such uncertainties as "confidence limits." The criterion is in the last analysis subjective: we would be "surprised" if the number in question fell outside of the quoted limits.

[51] This is a conservative estimate based on the difference in the result of extrapolations using t_c's which differ by 0.10–0.15%.

$\lambda=1$. There is evidence, as already suggested in Sec. 4 A, that the series are not fully asymptotic in the region of the dip, $0.6\lesssim\lambda<1$. In Fig. 3, for the case of prolate anisotropy, the values of $g_n=(\gamma-1)_n$, calculated from Eq. (3.9) applied to χ_z, are plotted versus $1/n$ for various values of λ. For $\lambda=0.2$, the points are quite linear and extrapolate to $g\approx0.23$. For $\lambda=0.6$, there is a break with an indication of a rapid increase in the g_n. For $\lambda=0.7$ and 0.8, there is indication that the curves will turn upward, but at $\lambda=0.9$ there is no indication. However, at $\lambda=1.0$ (Heisenberg limit, not shown) the curve is again quite linear (comparable to $\lambda=0.2$), extrapolating to $g\approx0.38$.[7,8] The oblate case behaves similarly. Figure 3 is taken as evidence that for $0.6\lesssim\lambda<1$ the true asymptotic behavior is not being reflected in the terms available. On the basis of this discussion, we surmise that *the critical indices γ and $2\nu_1$ are constant for all prolate (oblate) anisotropies at their Ising (x-y) values and change discontinuously at the discrete point $\lambda=1$ to the isotropic Heisenberg values.*[52] It is interesting to note that this step-function behavior for γ was found by Dalton and Wood[18] for the spin-$\frac{1}{2}$ prolate Heisenberg model in the random-phase approximation.

With this understanding of Table III, we proceed to examine the more complex combinations of anisotropy parameters represented in Table IV. We propose that three sets of critical indices are sufficient to characterize the dominant singularities for all cases we have been

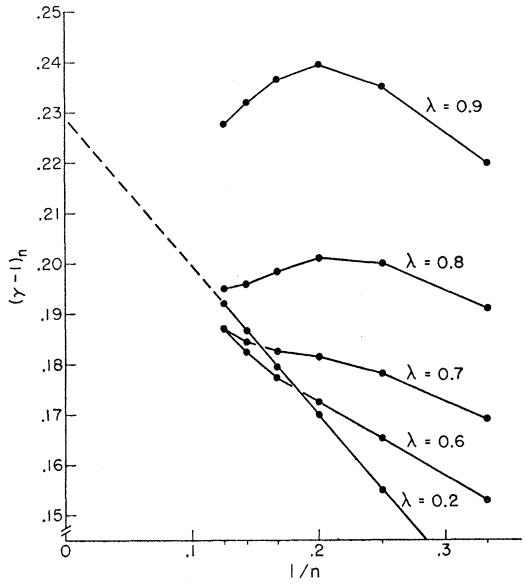

FIG. 3. The sequences $\{g_n\}$, defined by Eq. (3.9) applied to χ_z versus $1/n$ for various values of λ in the case of prolate anisotropy. From (3.5), $\{g_n\}\to(\gamma-1)$.

[52] In this light, the characteristic overshoot of the region $0.6\lesssim\lambda<1$ seems like a kind of Gibbs phenomenon and would most likely disappear from the left as more terms in the series became available. Each coefficient in the series is a finite polynomial in λ. The ρ_n's and, therefore, the critical indices must vary smoothly with λ except in the limit $n\to\infty$.

TABLE IV. Indices γ and $2\nu_1$ for various typical combinations of the anisotropy parameters.[a]

	η_x	η_y	η_z	Comp.	γ	$2\nu_1$
1	0.1	0.5	1.0	z	1.23	1.25
2	0.2	0.5	1.0	z	1.23	1.25
3	0.4	0.5	1.0	z	1.23	1.25
4	0.5	−0.5	1.0	z	1.225	1.245
5	−0.5	−0.5	1.0	z	1.225	1.25
6	0.4	−0.5	1.0	z	1.225	1.245
7	1.0	1.0	−0.5	x	1.31	1.33
8[b]	1.0	0.75	0.0	x	1.21	1.23
9	1.0	0.2	0.0	x	1.23	1.25
10[c]	1.0	−1.0	0.0	x	1.23	1.24
					(1.32)	(1.34)
11[c]	1.0	1.0	−1.0	x	1.32	1.33
					(1.38)	(1.40)
12[c]	1.0	−1.0	−1.0	x	1.23	1.24
					(1.38)	(1.40)

[a] Unless otherwise noted, confidence limits are ±1%.
[b] No confidence limits given; series not showing asymptotic behavior.
[c] bcc indices in parenthesis, confidence limits ±1.5%; fcc confidence limits ±1.5–2.0%.

able to analyze.[53] We will refer to these as

$$\text{Ising-like:}\qquad \gamma=1.23,\ 2\nu_1=1.25, \tag{4.1a}$$

$$x\text{-}y\text{-like:}\qquad \gamma=1.32,\ 2\nu_1=1.34, \tag{4.1b}$$

$$\text{Heisenberg-like:}\qquad \gamma=1.38,\ 2\nu_1=1.40, \tag{4.1c}$$

with confidence limits of ±1%. Which of these sets of indices is to be associated with a given set of anisotropy parameters appears to be determined by the lattice type and the relative magnitudes and signs of the η_α's as shown in Table V. Note how the entries of Table IV fit into the scheme of Table V. For example, the first six entries of Table IV have a dominant z-coupling which is ferromagnetic and give Ising-like indices in accordance with Table V, A(i). The confidence limits shown in (4.1) refer to the well-behaved cases. When, as in Table IV (8) one nears the discontinuity of the step-function, one observes the characteristic overshoot phenomenon mentioned above and in Ref. 52. Correspondingly, the series indicate internally that they are not yet fully asymptotic, and our critical exponent estimates are expected to be unreliable, as discussed in connection with the simple prolate and oblate anisotropies of Table III. In addition the cases [e.g., Table IV(10–12)] where the dominant anisotropy parameters have mixed signs are quite difficult to extrapolate. Confidence limits in these cases are correspondingly wider; it does seem possible to assign these cases unambiguously to one of the three categories (4.1a)–(4.1c).

When the dominant anisotropy parameters are all positive [Table V—A(i), B(i), C(i)], there are no lattice effects. In other cases, there are marked dif-

[53] In the specific (fcc) case when all dominant couplings are antiferromagnetic the series are not sufficiently regular to analyze reliably. See below, Table V, and Appendix B. All other cases are covered by the indices (4.1).

TABLE V. Critical indices and ground-state behavior as functions of the anisotropy parameters.

Anisotropy parameters: Magnitudes	Anisotropy parameters: Signs	Indices and[a] ground state: fcc	Indices and[a] ground state: bcc	Component studied
A. $\lvert\eta_z\rvert > \lvert\eta_x\rvert, \lvert\eta_y\rvert$	(i) $\eta_z>0$	I	I	z
	(ii) $\eta_z<0$	?	I	? (z^s)
B. $\lvert\eta_x\rvert = \lvert\eta_y\rvert > \lvert\eta_z\rvert$	(i) $\eta_x, \eta_y>0$	xy	xy	x, y
	(ii) $\eta_x>0; \eta_y<0$	I	xy	$x(y^s)$
	(iii) $\eta_x, \eta_y<0$	?	xy	?(x^s, y^s)
C. $\lvert\eta_x\rvert = \lvert\eta_y\rvert = \lvert\eta_z\rvert$	(i) $\eta_x, \eta_y, \eta_z>0$	H	H	x, y, z
	(ii) $\eta_x, \eta_y>0; \eta_z<0$	xy	H	$x, y(z^s)$
	(iii) $\eta_z>0; \eta_x, \eta_y<0$	I	H	$z(x^s, y^s)$
	(iv) $\eta_x, \eta_y, \eta_z<0$	?	H	?(x^s, y^s, z^s)

[a] I="Ising-like"; xy="x-y-like"; H="Heisenberg-like" (isotropic). See Eq. (4.1). The notation α^s refers to the staggered version of the α component. Parenthesized quantities were studied on the bcc lattice only.

ferences between fcc and bcc behavior. The fact that the indices for the bcc lattice do not depend upon the sign of the anisotropy parameters is a consequence of a general symmetry for loose-packed lattices[54]:

$$\chi_x(\eta_x, \eta_y, \eta_z) = \chi_x(\eta_x, \pm\eta_y, \pm\eta_z)$$

and

$$\chi_x(-\eta_x, \eta_y, \eta_z) = \chi_x{}^s(\eta_x, \pm\eta_y, \pm\eta_z), \qquad (4.2)$$

which holds for any combination of the $\pm$ signs. $\chi_\alpha{}^s$ refers to the staggered susceptibility,[55]

$$\chi_\alpha{}^s = \sum_2 P(12)\mathfrak{M}_{\alpha\alpha}(12),$$

where

$$\begin{aligned} P(12) &= 1, && \text{1 and 2 on same sublattice,} \\ &= -1, && \text{1 and 2 on different sublattices.} \end{aligned} \qquad (4.3)$$

Consider, for example, the case B(ii) of Table V for the bcc lattice:

$$\begin{aligned} \chi_x(\eta_x, \eta_y, \eta_z) &= \chi_x(\eta_x, \lvert\eta_y\rvert, \eta_z) \\ &= \chi_y(\eta_z, \lvert\eta_y\rvert, \eta_z) \\ &= \chi_y{}^s(\eta_x, \eta_y, \eta_z), \end{aligned} \qquad (4.4)$$

where the first and third equality signs depend on (4.2), while the second expresses rotational symmetry in the x-y plane. Thus, for this case, the series for χ_x and $\chi_y{}^s$ are identical not only with each other (as indicated in the "component" column of Table V) but also with the susceptibility $\chi_x(\eta_x, \lvert\eta_y\rvert, \eta_z)$, which falls into category B(i). The dominant singularities in the bcc antiferromagnetic cases A(ii), B(iii), C(iv) are entirely in the staggered susceptibilities, and it is the index of these singularities which we identify with γ. The much weaker physical susceptibilities (which are, of course, the staggered susceptibilities of the corresponding ferromagnets) are entirely masked.[56]

It is a remarkable empirical fact that the classification of the critical indices in their dependence on the anisotropy parameters (as given in Table V) *exactly* parallels the classification of ground-state symmetry (degeneracy) as a function of anisotropy parameters. For most[57] combinations of anisotropy parameters the ground state of the Hamiltonian (2.1) subject to (2.2) can be obtained from entirely elementary arguments, as outlined in Appendix B. When these arguments go through—and they do go through for just those cases in which our series are analyzable—they predict three different types of ground-state structure: (a) Ising-like, in which the ground state is doubly degenerate with respect to a coherent flipping of every spin in the lattice, (b) x-y-like, in which the ground state is degenerate with respect to a coherent planar rotation of every spin, and (c) isotropic-Heisenberg-like, in which the ground state is degenerate with respect to a coherent three-dimensional rotation of every spin. The cases (a)–(c) above are in exact correspondence with the occurrence of the indices (4.1a)–(4.1c). (For the close-packed lattices with dominant antiferromagnetic coupling the ground state has a more complex structure.[58]) This, then, is the content of the hypothesis stated in the Introduction.

[54] Equation (4.2) holds for the Hamiltonian (2.1) under conditions (2.2) for $T>T_c$ on any lattice admitting a two-sublattice structure. A change in sign $\eta_\alpha \to -\eta_\alpha$ for any given α can be compensated by a corresponding change of variable $S_\alpha(1) \to -S_\alpha(1)$ on one of the two sublattices. There is no loss of generality for the loose-packed lattices in taking $\eta_\alpha \geq 0$. The generality of this result depends on the fact that we are dealing with *classical* spins. For finite spin there is an analogous but restricted relation involving simultaneous sign changes of two anisotropy parameters.

[55] G. S. Rushbrooke and P. J. Wood, Mol. Phys. **6**, 409 (1963). A staggered second moment can be defined similarly.

[56] We have attempted to remove the strong singularity in a manner similar to that used by M. E. Fisher and M. F. Sykes, Physica **28**, 939 (1962), for the $S=\frac{1}{2}$ Ising model. The resulting series were not analyzable.

[57] The exception is for the close-packed lattices when the dominant anisotropy parameters are all negative, cf. Ref. 53.

[58] Examples in the context of the $S=\frac{1}{2}$ Ising model may be found in Ref. 3 (G. Wannier) and D. D. Betts and C. J. Elliott, Phys. Letters **18**, 18 (1965).

C. Specific Heat: α

The specific-heat series are very difficult to analyze. The loose-packed lattices cannot be used here because the odd terms in the series vanish, leaving too few to extrapolate reliably. For the fcc lattice the specific-heat index behaves with respect to symmetry just as γ and ν_1 do, and for the important limits,

$$\begin{aligned} &\alpha \cong +0.1, && (S=\infty \text{ Ising}) \text{ (Ref. 15)} \\ &\alpha \cong 0, && (\text{classical } x\text{-}y) \\ &\alpha_s \cong -0.1 && (\text{classical Heisenberg}), \end{aligned} \tag{4.5}$$

where α_s is the index for the singular part of the specific heat. In (4.5) reasonable confidence limits for the extrapolations might be as large as ± 0.1. In each case quoted in (4.5) the specific heat $C_{H=M=0}$ is either equal to or proportional to the nonvanishing component(s), C_α, defined in (2.8c). In other cases both the total specific heat and the components were considered. Generally the component which yields the most singular (and most regular) χ and μ_2 series also yields the smoothest specific-heat component. The other components are, in comparison, numerically small and slightly retard convergence of the total specific-heat series.

The results indicate that the specific heat of the classical Heisenberg model may be finite,[7] in agreement with the latest results[6] for the $S=\frac{1}{2}$ case. There is an indication of the possibility that the x-y model has a logarithmic specific heat.

D. Comment on the S = ∞ Ising Model

For this model our series are the longest that have been derived to date. We find quite convincing differences between the indices of this model and the $S=\frac{1}{2}$ Ising model. These differences are summarized in (4.6) for the three-dimensional lattices.[59]

$$\begin{aligned} &\gamma_{1/2}=1.250\pm 0.002, && \gamma_\infty \cong 1.23\pm 1\%, \\ &2\nu_{1/2}=1.286\pm 0.005, && 2\nu_\infty \cong 1.25\pm 1\%. \end{aligned} \tag{4.6}$$

Recalling the tables of results (see also Table II), we consistently find, for cases with Ising-like ordering, values of γ and $2\nu_1$ lower than the $S=\frac{1}{2}$ results. Results for the general spin Ising model have now been extended to ten terms.[60]

[59] See Ref. 17. We have added two terms to their μ_2 (fcc), and have corrected a small error in the eighth and added the ninth term in μ_2 (bcc). M. Moore, D. Jasnow, M. Wortis (to be published). Using the most recent estimates for T_c (fcc) in M. F. Sykes, J. L. Martin, and D. L. Hunter, Proc. Phys. Soc. (London) **91**, 671 (1967), might cause the lowering of the estimate, for $2\nu_{1/2}$ in (4.8) by a few tenths of a percent.

[60] M. Moore, D. Jasnow, M. Wortis (to be published).

5. DISCUSSION

In the context of the anisotropic classical Heisenberg model, the results provide some information in relation to the questions (a) and (b) posed in the Introduction. We find three sets of critical indices. The anisotropy parameters can be varied, altering the dynamical situation, without changing the critical indices, as long as the ground-state manifold does not change. That is to say, the cases which could be treated[53,57] indicated that the interactions matter only insofar as they determine the symmetry of the order parameter in the ground state. If, as is plausible, the order parameter has the same symmetry for $T<T_c$ as it does at $T=0$, the results correlate the high-temperature critical indices with the symmetry of the ordered phase.

An interesting comparison can be made between our x-y-like models and the model of interacting two-dimensional classical unit vectors [Hamiltonian (2.1) with $\alpha=x, y$ and $S(1)=(S_x(1), S_y(1))$].[61] Bowers and Joyce[62] find for the isotropic limit of such a model on three-dimensional lattices indices γ and α in excellent agreement with the values we quote for the x-y-like models. The difference between the models is one of phase space; the ground-state manifolds are identical. Work is in progress to determine ν_1 for the "planar" model.[35]

Several comments can be made on the relation of our numerical results to the scaling laws.[63] Dropping the distinction between ν and ν_1, we can comment on

$$\gamma=(2-\eta)\nu \tag{5.1}$$

and

$$d\nu=2-\alpha, \tag{5.2}$$

where d is the dimensionality of the lattice. In the first place, the results (4.1a)–(4.1c) all indicate that $2\nu>\gamma$, implying a small positive value of η. However, γ and 2ν differ by roughly 2%, and, as stated previously, we have confidence in our values for each of these quantities to about $\pm 1\%$. Hence the possibility that $\eta\equiv 0$ is not out of the question, although numerically we find a consistent slight difference between γ and 2ν, suggesting $\eta\cong 0.02$–0.03.

Our estimates of α are admittedly imprecise (possibly ± 0.1), but, taken at face value, (5.2) is remarkably well satisfied for our three sets of indices (4.1a)–(4.1c) and (4.7) [using α_s in (5.2) for the Heisenberg limit]. Recall that the $S=\frac{1}{2}$ three-dimensional Ising model presents a difficulty with respect to (5.1) and (5.2), since $\alpha=\frac{1}{8}$ and $\gamma=\frac{5}{4}$ implies $\eta=0$ and $2\nu=\gamma$. The last equality does not appear to be the case.[17,59] The

[61] V. G. Vaks and A. I. Larkin, Zh. Eksperim. i Teor. Fiz. **49**, 975 (1965) [English transl.: Soviet Phys.—JETP **22**, 678 (1966)] proposed this as a lattice model of the λ transition of liquid He^4.

[62] R. G. Bowers and G. S. Joyce, Phys. Rev. Letters **19**, 630 (1967). See also H. E. Stanley, Phys. Rev. Letters **20**, 150 (1968).

[63] L. P. Kadanoff, Physics **2**, 263 (1966); B. Widom, J. Chem. Phys. **43**, 3898 (1965).

results of this work, on the other hand, indicate that the $S=\infty$ Ising model (and, indeed, all cases considered) are consistent with the relations (5.1) and (5.2). As stated in Sec. 4, the series for the $S\neq\frac{1}{2}$ Ising models (and μ_2 for $S=\frac{1}{2}$) are being extended. In view of present problems with scaling theory, more precise estimates of α and ν will be most useful.

ACKNOWLEDGMENTS

The authors would like to thank Professor M. E. Fisher for helpful suggestions and comments, and Professor L. P. Kadanoff for his continued interest and many helpful conversations throughout the course of this work. Special thanks go to M. A. Moore for his independent checks on some of the calculations and frequent valuable discussions concerning various aspects of the analysis. One of us (D. J.) would like to express his gratitude to National Aeronautics and Space Administration and Eastman Kodak Co. for fellowship support.

APPENDIX A: SELECTED ZERO-FIELD SUSCEPTIBILITY AND SECOND-MOMENT COEFFICIENTS (fcc LATTICE)

	$\eta_x=\eta_y=0, \eta_z=1$		$\eta_x=\eta_y=0.5, \eta_z=1$	
n	a_n^z	b_n^z	a_n^z	b_n^z
1	1.3333	1.3333	1.3333	1.3333
2	5.0667	10.6667	5.0222	10.6667
3	18.8800	61.9022	18.5007	61.5526
4	69.4866	313.6000	67.2977	309.2069
5	253.6484	1 471.3803	242.8131	1 436.7542
6	920.5347	6 569.0511	871.0947	6 348.4609
7	3 326.3463	28 321.6706	3 111.8314	27 079.6495
8	11 979.5328	118 979.2153	11 079.9968	112 529.7574

	$\eta_x=\eta_y=1, \eta_z=1$		$\eta_x=\eta_y=1, \eta_z=0$	
n	a_n^z	b_n^z	a_n^x	b_n^x
1	1.3333	1.3333	1.3333	1.3333
2	4.8889	10.6667	4.9778	10.6667
3	17.2444	60.5037	18.0622	61.2030
4	59.4864	295.1111	64.4301	304.3556
5	202.2485	1 319.7991	227.2428	1 395.0621
6	680.7001	5 576.1756	795.1252	6 063.7043
7	2 273.9843	22 628.6321	2 765.7862	25 385.7514
8	7 553.1203	89 102.6500	9 576.8911	103 345.8207

$$\chi_\alpha(\eta_x,\eta_y,\eta_z)=\tfrac{1}{3}+\sum_{n=1} a_n^\alpha v^n$$

$$\mu_2^\alpha(\eta_x,\eta_y,\eta_z)=\sum_{n=1} b_n^\alpha v^n$$

APPENDIX B: DETERMINATION OF THE GROUND STATE

The ground-state structure can be simply determined if and only if the pair ground state of two coupled spins can be *coherently* imposed over the entire lattice for *every* nearest-neighbor pair. The basic problem, then, is to maximize $\sum_\alpha \eta_\alpha S_\alpha S_\alpha'$ subject to the subsidiary conditions $\sum_\alpha S_\alpha^2=\sum_\alpha S_\alpha'^2=1$. By the method of Lagrange multipliers, we are lead to extremize the quadratic form

$$\sum_\alpha[\eta_\alpha S_\alpha S_\alpha'-\tfrac{1}{2}\lambda_1 S_\alpha^2-\tfrac{1}{2}\lambda_2 S_\alpha'^2]. \tag{B1}$$

This gives

$$\eta_\alpha S_\alpha'=\lambda_1 S_\alpha \quad \text{and} \quad \eta_\alpha S_\alpha=\lambda_2 S_\alpha'. \tag{B2}$$

It follows from (B2) that

$$\sum_\alpha \eta_\alpha S_\alpha S_\alpha'=\lambda_1=\lambda_2=\lambda \tag{B3}$$

and that, if

$$\eta_\alpha^2\neq\lambda^2, \quad \text{then} \quad S_\alpha=S_\alpha'=0. \tag{B4}$$

If the subsidiary conditions are to be satisfied, there must be at least one α for which $\eta_\alpha^2=\lambda^2$. It, therefore, follows from (B3) that the very best we can hope for is $\sum_\alpha \eta_\alpha S_\alpha S_\alpha'=|\eta_{\max}|$, where $\eta_{\max}$ is the largest in absolute magnitude of the η_α's. A short computation shows that this maximum can always be achieved by choosing

$$S_\alpha=\operatorname{sgn}(\eta_\alpha)S_\alpha', \quad \text{for all } \alpha \text{ such that } |\eta_\alpha|=|\eta_{\max}|$$
$$=0, \quad \text{otherwise,} \tag{B5}$$

where $\operatorname{sgn}(x)=\pm 1$ for $x\gtrless 0$. (B5) constitutes the solution of the two-spin problem, and we note that, even after application of the normalization condition, there still remains an up-down (Ising-like), planar rotation (x-y-like), and three-dimensional rotation (isotropic, Heisenberg-like) degeneracy according as the maximal anisotropy parameter in absolute value is unique, doubly degenerate, or triply degenerate, respectively.

For the bcc lattice (or any loose-packed lattice) the sublattice structure guarantees that (B5) can be applied coherently, thus giving the ground state for the entire lattice as indicated in Table V.

For the fcc lattice, on the other hand, nearest neighbors of a given site can, themselves, be nearest neighbors. Thus, (B5) *cannot* be imposed coherently without the *additional* requirement that

$$S_\alpha=S_\alpha'=0, \qquad \text{whenever } \eta_\alpha<0. \tag{B6}$$

This further condition reduces the degeneracy for the entire lattice as shown in Table V for the fcc. Note that, when *all* the maximal anisotropy parameters are negative (antiferromagnetic), (B5) and (B6) together require $\mathbf{S}=\mathbf{S}'=0$, which is incompatible with normalization. In this case, our simple argument fails, and the ground state has a more complex structure.